

Analytical Bounds for Nonasymptotic Asymmetric State Discrimination

Jason L. Pereira^{1,2,*}, Leonardo Banchi^{1,3} and Stefano Pirandola¹

¹*Department of Computer Science, University of York, York YO10 5GH, United Kingdom*

²*Department of Physics and Astronomy, University of Florence, via G. Sansone 1, Sesto Fiorentino FI I-50019, Italy*

³*INFN Sezione di Firenze, via G. Sansone 1, Sesto Fiorentino, FI I-50019, Italy*

(Received 20 July 2022; revised 2 April 2023; accepted 3 April 2023; published 9 May 2023)

Two types of errors can occur when discriminating pairs of quantum states. Asymmetric state discrimination involves minimizing the probability of one type of error, subject to a constraint on the other. We give explicit expressions bounding the set of achievable errors, using the trace norm, the fidelity, and the quantum Chernoff bound. The upper bound is asymptotically tight and the lower bound is exact for pure states. Unlike asymptotic bounds, our bounds give error values instead of exponents, so can give more precise results when applied to finite-copy state discrimination problems.

DOI: 10.1103/PhysRevApplied.19.054030

I. INTRODUCTION

Suppose we want to carry out one-shot discrimination between a pair of quantum states, ρ_1 and ρ_2 . There are two types of errors that we are interested in. The Type I error, which we call α , is the probability of identifying the state as ρ_2 when it is actually ρ_1 , whilst the Type II error, which we call β , is the probability of identifying the state as ρ_1 when it is actually ρ_2 . There are two basic paradigms of quantum state discrimination: symmetric discrimination, where the aim is to minimize the average measurement error probability; and asymmetric discrimination, where the aim is to minimize the probability of one type of error subject to a constraint on the other.

In the symmetric setting the optimal error probability is given by the Helstrom theorem [1] and depends on the trace distance between ρ_1 and ρ_2 , which can be bounded using the fidelity, via the Fuchs-van der Graaf inequalities [2], or using the quantum Chernoff bound (QCB) [3]. For asymmetric discrimination, we have the quantum Neyman-Pearson relation [4], which gives the minimum weighted average of the two error types, and thus, implicitly lets us find the boundary of the set of achievable errors.

Asymmetric discrimination is needed in situations where one type of error is more undesirable than the other, and is ubiquitous in quantum information. In terms

of applications, asymmetric state discrimination is the central model adopted in many protocols of quantum sensing and quantum metrology, including quantum target detection [5–22], quantum reading of memories [23–35], quantum-enhanced pattern recognition [36], quantum-enhanced detection of bacterial growth [37], quantum-enhanced optical superresolution [38–53], etc, where it is often more important to avoid false negatives (fail to spot a target that is present) than false positives (detect a target when none is present). It is also central in the theory of quantum communications [54,55]. The decoding capabilities for receivers in quantum communications (e.g., cryptographic) scenarios are directly related to how well they can perform quantum measurements.

Asymmetric state discrimination has largely (though not exclusively [56,57]) been studied in the asymptotic regime, where the aim is to find the maximum exponent for the decay rate of one error type, subject to a constraint on the other. This problem has been solved, via the quantum Stein's lemma [58–61] and the quantum Hoeffding bound [62,63]. These results, however, tell us nothing about the actual values of the two types of errors, only the rates at which they decay. Finite-size analysis is a more realistic treatment for the practical implementation of a number of quantum information protocols.

One-shot expressions for α and β can be numerically computed using the hypothesis testing quantum relative entropy, which requires solving a semidefinite program [57]. However, numerical calculations become difficult for high-dimensional systems and scale exponentially with the number of copies. Moreover, such calculations are impossible for continuous-variable (CV) systems, such as Gaussian states. Ref. [57] also gives a lower bound on

*jason.pereira@fi.infn.it

Published by the American Physical Society under the terms of the [Creative Commons Attribution 4.0 International license](#). Further distribution of this work must maintain attribution to the author(s) and the published article's title, journal citation, and DOI.

the optimal errors, based on the quantum relative entropy (QRE), which is applicable when the QRE is finite and can be computed for Gaussian states [55]. See the appendices for more information.

In this paper we find the upper bound (UB) and lower bound (LB) for α and β in terms of the fidelity between ρ_1 and ρ_2 . We also find an upper bound based on the QCB. Our bounds have several advantages: (i) they can be computed efficiently for Gaussian states, using known expressions for the fidelity [64] and QCB [65]—this is crucial for applications such as quantum radar [5,10,18]; (ii) they can be applied without additional computational cost to situations involving multicopy states, since both the fidelity and the QCB can be expressed in terms of their single-copy values; (iii) our QCB bound is asymptotically tight, as it saturates the quantum Hoeffding bound, while the fidelity bound is exact for pure states. Unlike previous results about the asymptotic regime, these bounds allow the receiver operating characteristic to be drawn for both one-shot and multishot discrimination between any pair of states. All proofs are in the appendices. A MATHEMATICA notebook containing implementations of the bounds is available as Supplemental Material [66].

II. BOUNDS ON OPTIMAL ASYMMETRIC DISCRIMINATION

For measurement operators Π_1 and Π_2 , where $\Pi_2 = \mathbf{I} - \Pi_1$, we can write $\alpha = \text{Tr}[\Pi_2 \rho_1]$ and $\beta = \text{Tr}[\Pi_1 \rho_2]$. In terms of an auxiliary parameter p , which lies in the range $0 \leq p \leq 1$, the errors are connected via the quantum Neyman-Pearson relation, which states that [4]

$$p\alpha + (1-p)\beta \geq p\alpha^* + (1-p)\beta^* = \frac{1-t_p}{2}, \quad (1)$$

where $\{\alpha^*, \beta^*\}$ are a pair of achievable errors that are optimal for a particular value of p , in that they minimize $p\alpha + (1-p)\beta$. Such minimization can be solved explicitly and the result written as a function of the trace norm

$$t_p = \|(1-p)\rho_2 - p\rho_1\|_1. \quad (2)$$

The optimal errors $\{\alpha^*, \beta^*\}$ are achieved by the positive operator-valued measure (POVM)

$$\Pi_1^* = \{(1-p)\rho_2 - p\rho_1\}_-, \quad \Pi_2^* = \{(1-p)\rho_2 - p\rho_1\}_+, \quad (3)$$

where $\{X\}_{+(-)}$ is the projector onto the positive (negative) eigenspace of X and where we assume $((1-p)\rho_2 - p\rho_1)$ is full rank—the general case is discussed in Appendix B.

We want explicit expressions for α^* and β^* that let us draw the boundary of the set of achievable error probabilities, rather than the implicit expression given in Eq. (1).

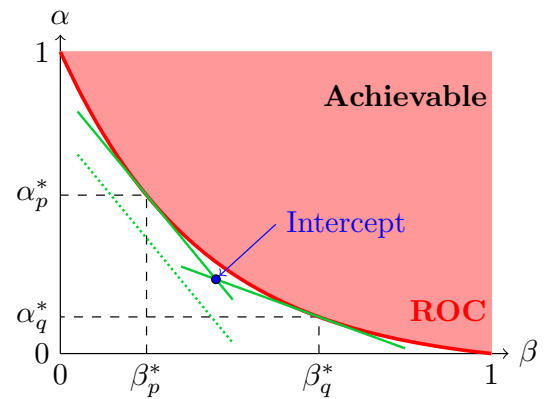


FIG. 1. The equation $p\alpha + (1-p)\beta = (1-t_p)/2$ defines a tangent to the ROC curve, which is parametrically defined as (β_p^*, α_p^*) for varying p . By considering two tangents (solid green lines) for different parameters p and q , and taking the limit $q \rightarrow p$, we can obtain from the intercept one point in the ROC curve, as given in Eq. (4).

Such a curve is called the receiver operating characteristic (ROC), and tells us the optimal Type I error for a given Type II error and vice versa. In Appendix A we show that α^* and β^* can be obtained from Eq. (2) and its derivative as

$$\alpha^* = \frac{1-t_p}{2} - \frac{1-p}{2} \frac{dt_p}{dp}, \quad \beta^* = \frac{1-t_p}{2} + \frac{p}{2} \frac{dt_p}{dp}. \quad (4)$$

A visual proof of the above equation is shown in Fig. 1. Because of the Neyman-Pearson relation (1) the tangents never pass above the ROC. Accordingly, the ROC curve is convex. For some states, there are values of p at which t_p is not differentiable, but we can still obtain a continuous ROC by replacing the derivative with the subgradient of the trace norm [67], as per Appendix B.

Suppose, instead of an expression for t_p , we have an expression that bounds t_p from either above or below. Can we use this to bound $\{\alpha^*, \beta^*\}$? We find that a lower bound on t_p gives an upper bound on the curve defining the boundary of achievable errors and an upper bound on t_p gives a lower bound—see, for instance, the dotted line in Fig. 1, which has a larger value of t_p . We are also guaranteed that if functions f_1 and f_2 both bound t_p from the same side, and f_2 is never tighter than f_1 , then f_1 gives a tighter bound on the set of achievable errors than f_2 . Finally, as long as the bounding functions are differentiable for all $0 < p < 1$, it does not matter if t_p is not differentiable for some values of p .

III. BOUNDS BASED ON THE FIDELITY

Let us bound t_p using Fuchs-van der Graaf style inequalities. Quantum fidelity is defined by $F(\rho_1, \rho_2) = \|\sqrt{\rho_1} \sqrt{\rho_2}\|_1$. Defining

$$t_p^{(\text{UB},F)} = \sqrt{1 - 4p(1-p)F(\rho_1, \rho_2)^2}, \quad (5)$$

$$t_p^{(\text{LB},F)} = 1 - 2\sqrt{p(1-p)}F(\rho_1, \rho_2), \quad (6)$$

we get the bounds $t_p^{(\text{LB},F)} \leq t_p \leq t_p^{(\text{UB},F)}$. If both states are pure, the upper bound is an equality.

Using these bounds, we get the expressions

$$\alpha^{(\text{LB},F)} = \frac{2(1-p)F^2 - 1 + \sqrt{1 - 4p(1-p)F^2}}{2\sqrt{1 - 4p(1-p)F^2}}, \quad (7)$$

$$\beta^{(\text{LB},F)} = \frac{2pF^2 - 1 + \sqrt{1 - 4p(1-p)F^2}}{2\sqrt{1 - 4p(1-p)F^2}}, \quad (8)$$

which provide a lower bound on the boundary of the set of achievable errors, and

$$\alpha^{(\text{UB},F)} = \frac{F}{2} \sqrt{\frac{1-p}{p}}, \quad \beta^{(\text{UB},F)} = \frac{F}{2} \sqrt{\frac{p}{1-p}}, \quad (9)$$

which provide an upper bound on the boundary of the set of achievable errors.

To eliminate p , we substitute the expressions for the bounds on β into the expressions for the bounds on α . The lower bound becomes

$$\alpha^{(\text{LB},F)} = \beta - 2\beta F^2 + F \left(F - 2\sqrt{(1-\beta)\beta(1-F^2)} \right), \quad (10)$$

whilst the upper bound becomes $\alpha^{(\text{UB},F)} = \frac{1}{4}F^2\beta^{-1}$. The lower bound meets the axes (of the ROC) at the points $(0, F^2)$ and $(F^2, 0)$, and is tight for pure states.

The upper bound $\alpha^{(\text{UB},F)}$ diverges to infinity as $p \rightarrow 0$ and $\beta^{(\text{UB},F)}$ diverges as $p \rightarrow 1$. This is nonphysical, because the maximum possible error probability is 1. Since points $(0, 1)$ and $(1, 0)$ are achievable and both the ROC and $\alpha^{(\text{UB},F)}$ are convex, we can improve the upper bound using the two tangents to $\alpha^{(\text{UB},F)}$ that pass through points $(0, 1)$ and $(1, 0)$ (one through each point)—see the dashed lines in Fig. 2. We get the tighter piecewise function

$$\alpha^{(\text{UB},F)} = \begin{cases} 1 - \frac{\beta}{F^2} & \text{for } 0 \leq \beta \leq \frac{F^2}{2}, \\ \frac{F^2}{4\beta} & \text{for } \frac{F^2}{2} \leq \beta \leq \frac{1}{2}, \\ (1-\beta)F^2 & \text{for } \frac{1}{2} \leq \beta \leq 1. \end{cases} \quad (11)$$

These bounds are illustrated in Fig. 2 for a particular pair of states with a fidelity of approximately 0.782.

IV. BOUNDS BASED ON THE QUANTUM CHERNOFF BOUND

Since the (nonlogarithmic) QCB gives a tighter lower bound on the trace distance than the Fuchs-van der Graaf

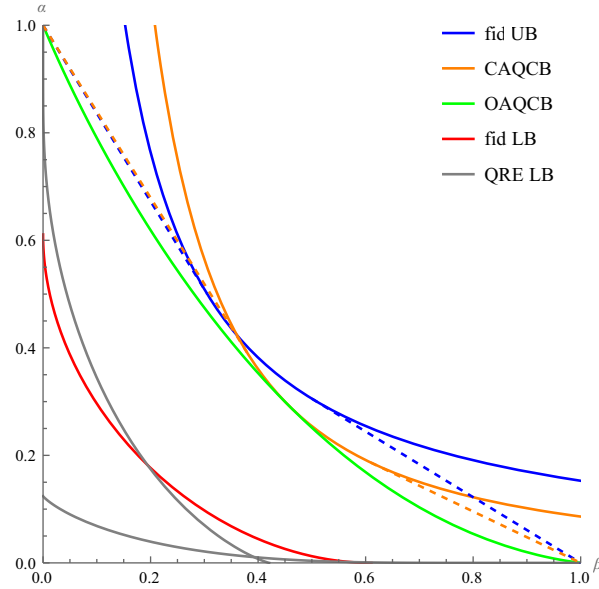


FIG. 2. ROC for discriminating between a pair of states, each the result of transmitting one mode of a two-mode squeezed vacuum, with an average photon number (per mode) of 4, through a thermal loss channel. Here ρ_1 (ρ_2) is obtained using a channel with a transmissivity of 0.7 (0.3) and a thermal number of 0.4 (0.6) [68]. The upper and lower bounds based on the fidelity are “fid UB” and “fid LB”, respectively. “CAQCB” is the upper bound obtained by setting $s_0 = s_*$ in Eq. (18). For the fidelity upper bound and the CAQCB, the solid lines are the original bounds, whilst the dashed lines are the piecewise modifications. “QRE LB” is an existing lower bound based on the QRE, from Ref. [57].

bound, we might suspect it could provide a tighter upper bound on the ROC. Defining

$$Q_s(\rho_1, \rho_2) = \text{Tr}[\rho_2^s \rho_1^{1-s}], \quad (12)$$

the QCB, Q_* , is given by

$$Q_* = Q_{s_*}, \quad s_* = \arg \min_{0 \leq s \leq 1} Q_s. \quad (13)$$

In Appendix D we show that

$$t_p \geq 1 - 2p^{1-s}(1-p)^s Q_s. \quad (14)$$

This defines a whole family of bounds. We are particularly interested in two scenarios: fixing s to some set value, $s = s_0$, and setting $s = s_{\text{opt}}$, the value of s that minimizes the right-hand side of Eq. (14). Note that s_* is a constant, while s_{opt} is a function of p . For constant $s = s_0$,

$$\alpha^{(\text{UB},s_0)} = \left(\frac{1-p}{p} \right)^{s_0} (1-s_0) Q_{s_0}, \quad (15)$$

$$\beta^{(\text{UB},s_0)} = \left(\frac{p}{1-p} \right)^{1-s_0} s_0 Q_{s_0}. \quad (16)$$

Eliminating p , we get

$$\alpha^{(\text{UB}, s_0)} = (1 - s_0)Q_{s_0}^{1/(1-s_0)} \left(\frac{s_0}{\beta} \right)^{s_0/(1-s_0)}. \quad (17)$$

In particular, we might consider setting $s_0 = s_*$, so that $Q_{s_0} = Q_*$ (the QCB).

This family of bounds (fixed $s = s_0$) diverges when one of the errors is small (similarly to the fidelity-based upper bound). We can again formulate piecewise bounds, using the tangents to these curves that pass through points $(0, 1)$ and $(1, 0)$,

$$\begin{aligned} \alpha^{(\text{UB}, s_0)} &= \\ &= \begin{cases} 1 - \beta Q_{s_0}^{-1/(1-s_0)}, & 0 \leq \beta \leq s_0 Q_{s_0}^{1/s_0}, \\ (1 - s_0)Q_{s_0}^{1/(1-s_0)} \left(\frac{s_0}{\beta} \right)^{s_0/(1-s_0)}, & s_0 Q_{s_0}^{1/s_0} \leq \beta \leq s_0, \\ (1 - \beta)Q_{s_0}^{1/(1-s_0)}, & s_0 \leq \beta \leq 1. \end{cases} \end{aligned} \quad (18)$$

We call this family of bounds the constant asymmetric QCBs (CAQCBs).

The bound obtained by setting $s = s_{\text{opt}}$ is

$$\alpha^{(\text{UB}, \text{QCB})} = \exp \left[-p Q_p^{-1} \frac{dQ_p}{dp} \right] (1 - p) Q_p, \quad (19)$$

$$\beta^{(\text{UB}, \text{QCB})} = \exp \left[(1 - p) Q_p^{-1} \frac{dQ_p}{dp} \right] p Q_p. \quad (20)$$

This is the optimal upper bound based on the QCB, so we call it the optimal asymmetric QCB (OAQCB).

Unlike the upper bound based on the fidelity or the CAQCBs, the OAQCB meets the axes at points $(0, Q_1)$ and $(Q_0, 0)$ (and $Q_s \leq 1$), so does not require piecewise modification. As demonstrated in Fig. 2, the OAQCB meets the CAQCB with s_0 set to s_* at the point $p = s_*$ (in fact, any CAQCB meets the OAQCB at $p = s_0$).

Explicit expressions for Gaussian states are provided in Appendix F, using results from Ref. [64].

V. MULTICOPY SCALING

Let us consider how the bounds scale for multicopy states. The two states we are discriminating between now take the form $\rho_1^{\otimes N}$ and $\rho_2^{\otimes N}$. We are interested in the scaling of the bounds with N .

The trace distance between multicopy states cannot be easily expressed in terms of the single-copy trace distance. On the other hand, both the fidelity and Q_s [as defined in Eq. (12)] are simply given by their single-copy values ($F_{(1)}$ and $Q_{s,(1)}$) to the power of N . We can write

$$F_{(N)} = F_{(1)}^N, \quad Q_{s,(N)} = Q_{s,(1)}^N. \quad (21)$$

This is one major benefit of using bounds based on the fidelity or the QCB rather than the trace norm.

For the bounds based on the fidelity, Eqs. (10) and (11), we replace F with $F_{(1)}^N$. We find the N -copy versions of the CAQCBs, Eqs. (17) and (18), in a similar way, by replacing Q_s with $Q_{s,(1)}^N$. For the OAQCB, we find that

$$\alpha_{(N)}^{(\text{UB}, \text{QCB})} = \frac{\left(\alpha_{(1)}^{(\text{UB}, \text{QCB})} \right)^N}{(1 - p)^{N-1}}, \quad (22)$$

$$\beta_{(N)}^{(\text{UB}, \text{QCB})} = \frac{\left(\beta_{(1)}^{(\text{UB}, \text{QCB})} \right)^N}{p^{N-1}}. \quad (23)$$

The quantum Hoeffding bound [62,63] asymptotically bounds the distinguishability of multicopy states. It constrains the maximum asymptotic decay rate of α , subject to a constraint on the asymptotic decay rate of β . For a family of discrimination tests on multicopy states, T_N , with corresponding Type I and II errors, $\{\alpha_N^\tau, \beta_N^\tau\}$, we define the Type I and II asymptotic decay rates as

$$\gamma_\alpha^\tau = \lim_{N \rightarrow \infty} \frac{-\ln [\alpha_N^\tau]}{N}, \quad \gamma_\beta^\tau = \lim_{N \rightarrow \infty} \frac{-\ln [\beta_N^\tau]}{N}. \quad (24)$$

The quantum Hoeffding bound then gives the maximum possible value of γ_α^τ , subject to a constraint on γ_β^τ ,

$$b_{\max}(r) = \sup_{\{\tau\}} \{ \gamma_\alpha^\tau | \gamma_\beta^\tau \geq r \} = \sup_{0 \leq s < 1} \frac{-sr - \ln [Q_{s,(1)}]}{1 - s}, \quad (25)$$

This bound is asymptotic and defines the best achievable scaling with the number of copies, but does not give actual values of $\{\alpha, \beta\}$. It holds for $0 < r < S(\rho_1 \| \rho_2)$, where S is the quantum relative entropy. Outside this range, the quantum Stein's lemma applies—see below.

Suppose we have a set of tests that achieve the OAQCB, with p fixed for all N . We calculate

$$\gamma_\alpha^{(\text{UB}, \text{QCB})} = p Q_{p,(1)}^{-1} \frac{dQ_{p,(1)}}{dp} - \ln [Q_{p,(1)}], \quad (26)$$

$$\gamma_\beta^{(\text{UB}, \text{QCB})} = -(1 - p) Q_{p,(1)}^{-1} \frac{dQ_{p,(1)}}{dp} - \ln [Q_{p,(1)}]. \quad (27)$$

Setting $r = \gamma_\beta^{(\text{UB}, \text{QCB})}$ in Eq. (25), we find that the maximum is obtained for $s = p$ and, hence,

$$b_{\max} \left(\gamma_\beta^{(\text{UB}, \text{QCB})} \right) = \gamma_\alpha^{(\text{UB}, \text{QCB})}, \quad (28)$$

showing the OAQCB achieves the best possible scaling, according to the quantum Hoeffding bound. Hence, the OAQCB is asymptotically tight, and any tighter upper bound has at most a subexponential advantage.

Next we consider the quantum Stein's lemma [58,59], which states that

$$\sup_{\{\mathcal{T}\}} \{ \gamma_\alpha^\mathcal{T} | \gamma_\beta^\mathcal{T} \geq 0 \} = S_{21}, \quad \sup_{\{\mathcal{T}\}} \{ \gamma_\alpha^\mathcal{T} | \gamma_\beta^\mathcal{T} = S_{12} \} = 0,$$

where $S_{ij} = S(\rho_i \| \rho_j)$. The maximum exponential rate at which the Type I error decreases with N such that the Type II error does not exponentially increase with N is given by the (single-copy) relative entropy.

We have shown that the OAQCB saturates the quantum Hoeffding bound; however, this is only applicable in the range $0 < r < S(\rho_1 \| \rho_2)$. We can show that it also saturates the quantum Stein's lemma.

Taking the limit of Eqs. (26) and (27) as $p \rightarrow 0$, we get

$$\gamma_{\alpha,p \rightarrow 0}^{(\text{UB,QCB})} = 0, \quad \gamma_{\beta,p \rightarrow 0}^{(\text{UB,QCB})} = S(\rho_1 \| \rho_2). \quad (29)$$

Taking the limit of Eqs. (26) and (27) as $p \rightarrow 1$, we get

$$\gamma_{\alpha,p \rightarrow 1}^{(\text{UB,QCB})} = S(\rho_2 \| \rho_1), \quad \gamma_{\beta,p \rightarrow 1}^{(\text{UB,QCB})} = 0. \quad (30)$$

Since $\gamma_{\beta(\alpha)}^{(\text{UB,QCB})}$ is a nonincreasing (nondecreasing) function of p , $0 \leq \gamma_{\beta}^{(\text{UB,QCB})} \leq S_{12}$, $0 \leq \gamma_{\alpha}^{(\text{UB,QCB})} \leq S_{21}$, for all values of the parameter p . Therefore, the OAQCB also saturates the quantum Stein's lemma.

VI. NONADAPTIVE AND ADAPTIVE MEASUREMENT SEQUENCES

Suppose we have one of two pure, N -copy states. We know the best possible Type I and II errors are given by Eqs. (7) and (8). We may ask whether these errors can be achieved with a sequence of single-copy measurements, i.e., by carrying out measurements on each copy individually, rather than collective measurements on multiple copies at once.

We consider two types of measurement sequences: nonadaptive sequences, in which the same measurement is carried out on each subsystem; and adaptive sequences, in which the measurement carried out on subsequent subsystems depends on the result of a measurement on a previous subsystem. We assume all of the single-copy measurements are optimal, i.e., have errors given by Eqs. (7) and (8), where F is the single-copy fidelity, $F_{(1)}$.

As an example for nonadaptive sequences, consider a three-copy state. We carry out three measurements—one on each subsystem—and use the results to decide which of two possible states we have. There are three main ways of combining the results to make our decision: decide we have $\rho_1^{\otimes 3}$ only if all three measurements tell us we have ρ_1 (case A), majority vote (case B), or decide we have $\rho_2^{\otimes 3}$ only if all three measurements tell us we have ρ_2 (case C). All three cases result in higher errors than the optimum, except at the points given by parameter values

$p = 0$ (where case A coincides with the optimum) and $p = 1$ (where case C coincides with the optimum)—see Appendix J for the exact expressions and a plot of the ROCs for each case.

Ref. [69] showed that the optimal measurement on a pure, multicopy state is achievable with an adaptive sequence of single-copy measurements. Ref. [70] made this more general by removing the requirement that each copy be identical.

Suppose we want to discriminate between a pair of pure states, ρ_1 and ρ_2 , that can be written as $\rho_i = \bigotimes_j^N \rho_{i,j}$, where $\rho_{1,j}$ and $\rho_{2,j}$ have the same dimension for all j . Both states can be partitioned into N subsystems in the same way (but $\rho_{i,j}$ and $\rho_{i,k}$ need not be identical copies). The optimal measurement can be achieved with an adaptive sequence of N measurements on each subsystem individually. The measurement on the next subsystem only depends on the result of the previous measurement (not the entire sequence of results).

Equations (7) and (8) give a simple, alternative way to show this result. Consider the two-subsystem states $\rho_i = \rho_{i,1} \otimes \rho_{i,2}$, where F_j is the fidelity between $\rho_{1,j}$ and $\rho_{2,j}$. Now consider a measurement sequence in which we carry out an optimal measurement [from the curve defined by Eqs. (7) and (8)], with parameter p_0 , on the first subsystem, then carry out another optimal measurement on the second subsystem, with the parameter depending on the previous measurement result. Here p_1^- (p_1^+) is the parameter if the first measurement tells us that the state is $\rho_{1,1}$ ($\rho_{2,1}$). Then, we use only the second measurement result to decide which state we have.

Using Eqs. (7) and (8) to calculate the error probabilities for the measurement sequence and setting

$$p_1^\mp = \frac{1}{2} \left(1 \mp \sqrt{1 - 4p_0(1 - p_0)F_1^2} \right), \quad (31)$$

we find that this sequence achieves the optimal errors for discriminating between states with a fidelity of $F_1 F_2$.

If the first subsystem can be partitioned into further subsystems, we can decompose the first measurement into a sequence of individual measurements on subsystems. In general, we choose a parameter, p_0 , for the measurement on the first subsystem and then measurements on the i th subsystem have a parameter value of

$$p_i^\mp = \frac{1}{2} \left(1 \mp \sqrt{1 - 4p_0(1 - p_0) \prod_{j=1}^{i-1} F_j^2} \right), \quad (32)$$

where the minus (plus) case is used when the $(i-1)$ th measurement indicates that the state is ρ_1 (ρ_2).

VII. CONCLUSION

We present explicit expressions for the Type I and II errors for discriminating between pairs of quantum states. Unlike asymptotic bounds, these expressions give actual values for the errors, rather than just error exponents. This could be useful for finite-copy scenarios, where the subexponential factors could be important. They give ultimate bounds on the performance of receivers, which can be applied to topics such as quantum target detection.

We give upper and lower bounds on the ROC based on the fidelity, and a family of upper bounds on it based on the QCB (the CAQCBs and the OAQCB). These bounds can be easily calculated analytically for a wide variety of states, including Gaussian states. It is simple to go from the single-copy expressions to multicopy expressions.

The fidelity lower bound and the OAQCB are of particular interest. Neither are trivial for any parameter value. The fidelity lower bound is exact for pure states, whilst the OAQCB saturates the quantum Hoeffding bound, so is asymptotically tight.

ACKNOWLEDGMENTS

J.L.P. and S.P. acknowledge funding from the European Union's Horizon 2020 Research and Innovation Action under grant agreement no. 862644 (FET-OPEN project: Quantum readout techniques and technologies, QUARTET). L.B. acknowledges funding from the U.S. Department of Energy, Office of Science, , Superconducting Quantum Materials and Systems Center (SQMS) under the Contract No. DE-AC02-07CH11359. The authors thank Marco Tomamichel for helpful correspondence.

APPENDIX A: DERIVATION OF BOUNDS ON THE RECEIVER OPERATING CHARACTERISTIC

The quantum Neyman-Pearson relation can be formulated in terms of a parameter p , constrained by $0 \leq p \leq 1$. We write

$$\begin{aligned} \mu_p &= p\alpha + (1-p)\beta \\ &= p\text{Tr}[\Pi_2\rho_1] + (1-p)\text{Tr}[(\mathbf{I} - \Pi_2)\rho_2] \\ &= \text{Tr}[p\Pi_2\rho_1 - (1-p)\Pi_2\rho_2] + (1-p)\text{Tr}[\rho_2] \\ &= 1 - p - \text{Tr}[\Pi_2((1-p)\rho_2 - p\rho_1)]. \end{aligned} \quad (\text{A1})$$

Here μ_p can be viewed as the average error probability for a measurement if the source emits state ρ_1 with probability p and state ρ_2 with probability $1 - p$. Minimizing μ_p over all operators $\Pi_2 \leq \mathbf{I}$, we find that the optimal value, μ_p^* , is achieved by the POVMs

$$\Pi_{1,p}^* = \{(1-p)\rho_2 - p\rho_1\}_-, \quad (\text{A2})$$

$$\Pi_{2,p}^* = \{(1-p)\rho_2 - p\rho_1\}_+ \quad (\text{A3})$$

(assuming $(1-p)\rho_2 - p\rho_1$ is full rank), and is equal to

$$\mu_p^* = 1 - p - \text{Tr}[((1-p)\rho_2 - p\rho_1)_+]. \quad (\text{A4})$$

By definition, $\text{Tr}[X] = \text{Tr}[(X)_+] - \text{Tr}[(X)_-]$, so

$$\begin{aligned} \text{Tr}[(1-p)\rho_2 - p\rho_1] &= \text{Tr}[((1-p)\rho_2 - p\rho_1)_+] \\ &\quad - \text{Tr}[((1-p)\rho_2 - p\rho_1)_-] \\ &= 1 - 2p. \end{aligned} \quad (\text{A5})$$

Similarly, $\|X\|_1 = \text{Tr}[(X)_+] + \text{Tr}[(X)_-]$, so

$$\begin{aligned} t_p &= \|(1-p)\rho_2 - p\rho_1\|_1 \\ &= \text{Tr}[((1-p)\rho_2 - p\rho_1)_+] \\ &\quad + \text{Tr}[((1-p)\rho_2 - p\rho_1)_-]. \end{aligned} \quad (\text{A6})$$

Combining Eqs. (A5) and (A6), we get

$$\text{Tr}[((1-p)\rho_2 - p\rho_1)_+] = \frac{1}{2}(1 - 2p + t_p), \quad (\text{A7})$$

and hence,

$$\mu_p^* = \frac{1}{2}(1 - t_p). \quad (\text{A8})$$

Thus, we can express μ_p^* in terms of t_p , the trace norm of $((1-p)\rho_2 - p\rho_1)$.

We therefore know that there exists some achievable pair of errors, $\{\alpha_p, \beta_p\}$, such that

$$p\alpha_p + (1-p)\beta_p = \frac{1}{2}(1 - t_p). \quad (\text{A9})$$

Furthermore, we know that there exists no pair of errors with a smaller value of μ_p . Therefore, the straight line (in a plot of α versus β)

$$\alpha = -\frac{1-p}{p}\beta + \frac{1-t_p}{2p} \quad (\text{A10})$$

defines a tangent to the boundary of the set of achievable errors for any value of p between 0 and 1. Any two such tangents will intersect at exactly one point. Two straight lines defined by $y = m_{1(2)}x + c_{1(2)}$ intersect at

$$x = \frac{c_2 - c_1}{m_1 - m_2}, \quad y = m_1 \frac{c_2 - c_1}{m_1 - m_2} + c_1. \quad (\text{A11})$$

Let us choose two values of p : p_0 and $p_0 + \delta$. The tangents for these two values of p will intersect at

$$\alpha_{\text{intersect}} = \frac{1 - t_{p_0}}{2} - \frac{1 - p_0}{2} \frac{t_{p_0+\delta} - t_{p_0}}{\delta}, \quad (\text{A12})$$

$$\beta_{\text{intersect}} = \frac{1 - t_{p_0}}{2} + \frac{p_0}{2} \frac{t_{p_0+\delta} - t_{p_0}}{\delta}. \quad (\text{A13})$$

By taking the limit as $\delta \rightarrow 0$, we get equations for α^* and β^* [Eq. (4) in the main text], the boundary values of the set

of achievable errors, in terms of the auxiliary parameter p ,

$$\alpha^* = \frac{1 - t_p}{2} - \frac{1 - p}{2} \frac{dt_p}{dp}, \quad \beta^* = \frac{1 - t_p}{2} + \frac{p}{2} \frac{dt_p}{dp}.$$

This can also be regarded as integrating the expression for the tangents with regard to p .

Suppose that, instead of having an expression for t_p , we have an expression that bounds t_p from either above or below. Swapping a lower bound on t_p for t_p in Eq. (A10) gives the tangent to the boundary of a set of pairs of errors that is contained by the set of achievable errors, and similarly swapping an upper bound on t_p for t_p gives the tangent to the boundary of a set of pairs of errors that contains the set of achievable errors (since it gives a line that is either a tangent to the set of achievable errors or is strictly below it). For the same reason, if functions f_1 and f_2 both bound t_p from the same side, and f_2 is never tighter than f_1 , then f_1 gives a tighter bound on the set of achievable errors than f_2 .

APPENDIX B: NONDIFFERENTIABLE TRACE NORM

Suppose the differential of the trace norm, t_p , does not exist for some values of p (note that t_p itself is continuous). How do we modify our expression for the ROC to accommodate this?

First, observe that discontinuities occur only when $(1 - p)\rho_2 - p\rho_1$ is not full rank, and that they are due to eigenvalues of $(1 - p)\rho_2 - p\rho_1$ “flipping” from negative to positive or vice versa. This follows from the fact that the eigenvalues of $(1 - p)\rho_2 - p\rho_1$ are differentiable functions of p , but the trace norm is the sum of their absolute values (and the gradient of the absolute value function has a discontinuity).

Since $(1 - p)\rho_2 - p\rho_1$ is not full rank, we must adjust the expressions for the POVM in Eqs. (A2) and (A3). They become

$$\Pi_{1,p,q}^* = \{(1 - p)\rho_2 - p\rho_1\}_- + q\Pi_0, \quad (\text{B1})$$

$$\Pi_{2,p,q}^* = \{(1 - p)\rho_2 - p\rho_1\}_+ + (1 - q)\Pi_0, \quad (\text{B2})$$

where $0 \leq q \leq 1$,

$$\Pi_0 = \{(1 - p)\rho_2 - p\rho_1\}_0, \quad (\text{B3})$$

and $\{X\}_0$ denotes the kernel of X . The remaining equations up to and including Eq. (A10) still apply (and are independent of the value of q). The difference is that the tangent given by Eq. (A10) now touches the ROC over a line segment rather than at a single point. This is because each value of q gives a different achievable pair of error values $\{\alpha_{p,q}, \beta_{p,q}\}$, but all with the same value of μ_p . Equation (A10) therefore gives the ROC for this segment (with p and t_p assessed at the discontinuity).

Note that the expression for the ROC given by Eq. (4) still applies for all values of p for which the differential of t_p exists. Consequently, we can draw the (piecewise) ROC by using Eq. (4) for all values of p for which the differential of t_p exists and joining up with a straight line segment the two points attained by taking the limit of Eq. (4) as p approaches the discontinuity from below and from above.

More precisely, calling $x_p = \text{tr}\{\Pi_0\rho_1\}$ and $y_p = \text{tr}\{\Pi_0\rho_2\}$, then by definition $(1 - p)y_p - px_p = 0$. Therefore, we may write

$$\alpha_{p,q}^* = \frac{1 - t_p}{2} - \frac{1 - p}{2} \frac{dt_p}{dp} + qx_p, \quad (\text{B4})$$

$$\beta_{p,q}^* = \frac{1 - t_p}{2} + \frac{p}{2} \frac{dt_p}{dp} + (1 - q) \frac{p}{1 - p} x_p. \quad (\text{B5})$$

Note that $x_p = 0$ as long as dt_p/dp is continuous. Suppose now that dt_p/dp has a discontinuity at \tilde{p} , then $\alpha_{\tilde{p}\pm}^*$ (as well as $\beta_{\tilde{p}\pm}^*$) are different (where $\tilde{p}\pm$ refers to p approaching \tilde{p} either from right or left). Since $x_{\tilde{p}} \neq 0$, we can vary q to join the left and right values. Indeed, $(\beta_{\tilde{p}-}, \alpha_{\tilde{p}-})$ and $(\beta_{\tilde{p}+}, \alpha_{\tilde{p}+})$ define two distinct points in the (β, α) plane, and we can vary q to join them with a straight line.

A simpler proof of the same result can be obtained by replacing the derivative dt/dp with the subgradient $\partial_p^q t_p$. The subgradient for the trace norm is calculated in Ref. [67]. When t_p is differentiable, then $\partial_p^q t_p = dt_p/dp$, namely the subgradient consists of a single point, the derivative. On the other hand, when dt_p/dp is discontinuous, the subgradient consists of a region, parameterized by q , that interpolates between the two discontinuous points

$$\partial_p^q t_p = \left. \frac{dt_p}{dp} \right|_{p-} q + \left. \frac{dt_p}{dp} \right|_{p+} (1 - q). \quad (\text{B6})$$

Writing

$$\alpha_{p,q}^* = \frac{1 - t_p}{2} - \frac{1 - p}{2} \partial_p^q t_p, \quad (\text{B7})$$

$$\beta_{p,q}^* = \frac{1 - t_p}{2} + \frac{p}{2} \partial_p^q t_p, \quad (\text{B8})$$

we see that we can use q to join the two discontinuous points in the (β, α) plane with a straight line.

Figure 3 gives the ROC for two examples of pairs of states for which t_p is discontinuous. The first is a pair of qubits that are diagonal in the same basis. Specifically, the density matrices of the states are

$$\rho_1 = \frac{1}{5} \begin{pmatrix} 4 & 0 \\ 0 & 1 \end{pmatrix}, \quad \rho_2 = \frac{1}{5} \begin{pmatrix} 3 & 0 \\ 0 & 2 \end{pmatrix}. \quad (\text{B9})$$

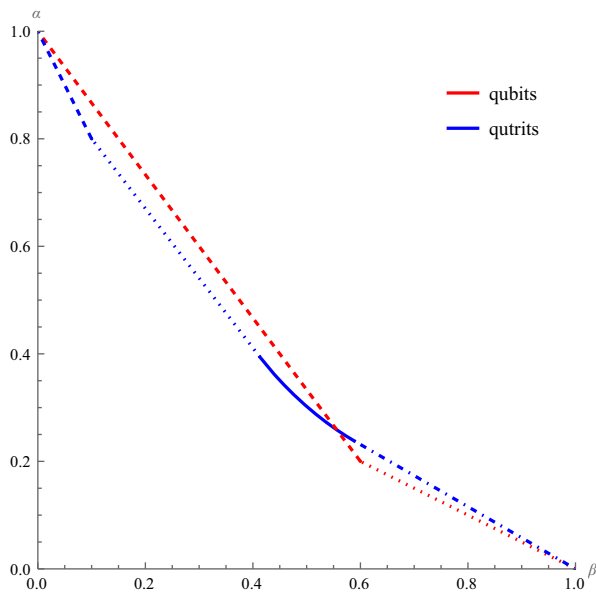


FIG. 3. The ROC for two discrimination problems that both involve a nondifferentiable (at points) trace norm, t_p . The qubit case involves a pair of qubit states that are diagonalizable in the same basis, whilst the qutrit case involves a pair of qutrit states that are not. The continuous line in the qutrit case is the part of the curve that corresponds to differentiable t_p , and is the only part of the ROC that is not a straight line.

The second is a pair of qutrits with density matrices

$$\rho_1 = \frac{1}{5} \begin{pmatrix} 3 & 0 & 0 \\ 0 & 1 & 0 \\ 0 & 0 & 1 \end{pmatrix}, \quad \rho_2 = \frac{1}{10} \begin{pmatrix} 6 & 1 & 1 \\ 1 & 2 & 1 \\ 1 & 1 & 2 \end{pmatrix}. \quad (\text{B10})$$

In the qubit case there are two discontinuities in the gradient of t_p (since there are two values of p for which one of the eigenvalues of $(1-p)\rho_2 - p\rho_1$ is equal to 0). These divide the interval $0 \leq p \leq 1$ into three regimes. However, we find that assessing Eq. (4) in each regime gives a single point with no p dependence in each case. We connect these three points with straight lines to get the curve in Fig. 3.

In the qutrit case there are three discontinuities and, hence, four regimes. However, in this case, in one of the regimes, α and β are not constant, but depend on p . We therefore have a segment of the ROC that is not a straight line.

APPENDIX C: DERIVATION OF BOUNDS BASED ON THE FIDELITY

We can bound t_p from above and below in terms of the fidelity, by proceeding similarly to the derivations for the $p = \frac{1}{2}$ case in Ref. [2].

Let ρ_1 and ρ_2 be a pair of states with fidelity F , and let $|\rho'_1\rangle$ and $|\rho'_2\rangle$ be purifications of ρ_1 and ρ_2 that have the same fidelity (these are guaranteed to exist by the definition

of fidelity). For any pair of positive semidefinite numbers, p and q , and any pair of quantum states, $|u\rangle$ and $|v\rangle$, we have the identity

$$\|p|u\rangle\langle u| - q|v\rangle\langle v|\|_1 = \sqrt{(p+q)^2 - 4pq|\langle u|v\rangle|^2}. \quad (\text{C1})$$

Therefore, we can write

$$\begin{aligned} &\|(1-p)|\rho'_2\rangle\langle\rho'_2| - p|\rho'_1\rangle\langle\rho'_1|\|_1 \\ &= \sqrt{1 - 4p(1-p)|\langle\rho'_2|\rho'_1\rangle|^2}. \end{aligned} \quad (\text{C2})$$

Then, since the trace norm is monotonic under partial tracing, we have the upper bound

$$t_p \leq \sqrt{1 - 4p(1-p)F(\rho_1, \rho_2)^2}. \quad (\text{C3})$$

If ρ_1 and ρ_2 are pure, this bound becomes an equality.

For any pair of positive semidefinite operators, X and Y , we can write

$$\|X - Y\|_1 \geq \left\| \sqrt{X} - \sqrt{Y} \right\|_2^2. \quad (\text{C4})$$

Consequently,

$$\begin{aligned} t_p &\geq \left\| \sqrt{1-p}\sqrt{\rho_2} - \sqrt{p}\sqrt{\rho_1} \right\|_2^2 \\ &\geq \text{Tr} \left[\left(\sqrt{1-p}\sqrt{\rho_2} - \sqrt{p}\sqrt{\rho_1} \right)^2 \right] \\ &\geq (1-p) + p - 2\sqrt{p(1-p)}\text{Tr}[\sqrt{\rho_1}\sqrt{\rho_2}] \\ &\geq 1 - 2\sqrt{p(1-p)}F(\rho_1, \rho_2). \end{aligned} \quad (\text{C5})$$

We define [Eqs. (5) and (6) in the main text]

$$\begin{aligned} t_p^{(\text{UB}, F)} &= \sqrt{1 - 4p(1-p)F(\rho_1, \rho_2)^2}, \\ t_p^{(\text{LB}, F)} &= 1 - 2\sqrt{p(1-p)}F(\rho_1, \rho_2). \end{aligned}$$

We can now differentiate both with regard to p . We get

$$\frac{dt_p^{(\text{UB}, F)}}{dp} = \frac{2(2p-1)F(\rho_1, \rho_2)^2}{\sqrt{1 - 4p(1-p)F(\rho_1, \rho_2)^2}}, \quad (\text{C6})$$

$$\frac{dt_p^{(\text{LB}, F)}}{dp} = \frac{(2p-1)F(\rho_1, \rho_2)}{\sqrt{p(1-p)}}. \quad (\text{C7})$$

Substituting Eqs. (5) and (6) and Eqs. (C6) and (C7) into Eq. (4), we get upper and lower bounds on the boundary

of the set of achievable errors [Eqs. (7) to (9) in the main text],

$$\begin{aligned}\alpha^{(\text{LB},F)} &= \frac{2(1-p)F^2 - 1 + \sqrt{1-4p(1-p)F^2}}{2\sqrt{1-4p(1-p)F^2}}, \\ \beta^{(\text{LB},F)} &= \frac{2pF^2 - 1 + \sqrt{1-4p(1-p)F^2}}{2\sqrt{1-4p(1-p)F^2}}, \\ \alpha^{(\text{UB},F)} &= \frac{F}{2} \sqrt{\frac{1-p}{p}}, \quad \beta^{(\text{UB},F)} = \frac{F}{2} \sqrt{\frac{p}{1-p}}.\end{aligned}$$

APPENDIX D: DERIVATION OF BOUNDS BASED ON THE QUANTUM CHERNOFF BOUND

From Ref. [3], we have that, for any pair of positive semidefinite operators, A and B , and any $0 \leq s \leq 1$,

$$\text{Tr}[A^s B^{1-s}] \geq \frac{1}{2} \text{Tr}[A + B - |A - B|]. \quad (\text{D1})$$

Substituting $(1-p)\rho_2$ for A and $p\rho_1$ for B and rearranging, we get

$$p^{1-s}(1-p)^s \text{Tr}[\rho_2^s \rho_1^{1-s}] + \frac{1}{2} \| (1-p)\rho_2 - p\rho_1 \|_1 \geq \frac{1}{2}. \quad (\text{D2})$$

Using the definition of Q_s , we can therefore write [Eq. (14) in the main text]

$$t_p \geq 1 - 2p^{1-s}(1-p)^s Q_s.$$

If we set $s = s_*$, Eq. (14) becomes

$$t_p \geq 1 - 2p^{1-s_*}(1-p)^{s_*} Q_*, \quad (\text{D3})$$

which we expect to be tighter than the inequality in Eq. (C5) for some values of p (in particular, close to $\frac{1}{2}$).

Note that this is not the tightest lower bound on t_p , since s_* minimizes Q_s rather than $p^{1-s}(1-p)^s Q_s$. The optimal value of s (achieving the tightest bound) is therefore not a constant, but is rather a function of p . We call this value s_{opt} , and define

$$Q_{\text{opt}} = Q_{s_{\text{opt}}}, \quad s_{\text{opt}} = \arg \min_{0 \leq s \leq 1} p^{1-s}(1-p)^s Q_s. \quad (\text{D4})$$

By differentiation, s_{opt} satisfies

$$\ln \left[\frac{1-p}{p} \right] Q_{\text{opt}} + \frac{dQ_s}{ds} \Big|_{s=s_{\text{opt}}} = 0. \quad (\text{D5})$$

If we have an analytical expression for Q_s in terms of s , we can analytically calculate $s_{\text{opt}}(p)$ (although we later show that finding $s_{\text{opt}}(p)$ is not necessary).

Defining the family of lower bounds on t_p as

$$t_p^{(\text{LB},s)} = 1 - 2p^{1-s}(1-p)^s Q_s, \quad (\text{D6})$$

and treating s as a function of p , we differentiate to get

$$\begin{aligned}\frac{dt_p^{(\text{LB},s)}}{dp} &= \frac{\partial t_p^{(\text{LB},s)}}{\partial p} + \frac{\partial t_p^{(\text{LB},s)}}{\partial s} \frac{ds}{dp} \\ &= -2 \frac{(1-p)^{s-1}}{p^s} \left((1-p-s)Q_s \right. \\ &\quad \left. + p(1-p) \frac{ds}{dp} \left(\ln \left[\frac{1-p}{p} \right] Q_s + \frac{dQ_s}{ds} \right) \right).\end{aligned} \quad (\text{D7})$$

We are interested in two scenarios in particular: fixing s to some set value, $s = s_0$, and setting $s = s_{\text{opt}}$. In the former case $ds/dp = 0$, and in the latter case $\partial t_p^{(\text{LB},s)}/\partial s = 0$. In both cases, Eq. (D7) reduces to

$$\frac{dt_p^{(\text{LB},s')}}{dp} = -2Q_{s'} \left(\frac{1-p}{p} \right)^{s'} \frac{1-p-s'}{1-p}, \quad (\text{D8})$$

where s' stands in for either s_0 or s_{opt} .

Substituting Eqs. (D6) and (D7) into Eq. (4), we get

$$\begin{aligned}\alpha^{(\text{UB},s)} &= \left(\frac{1-p}{p} \right)^s \left[(1-s)Q_s \right. \\ &\quad \left. + p(1-p) \frac{ds}{dp} \left(\ln \left[\frac{1-p}{p} \right] Q_s + \frac{dQ_s}{ds} \right) \right],\end{aligned} \quad (\text{D9})$$

$$\begin{aligned}\beta^{(\text{UB},s)} &= \left(\frac{p}{1-p} \right)^{1-s} \left[sQ_s \right. \\ &\quad \left. + p(1-p) \frac{ds}{dp} \left(\ln \left[\frac{p}{1-p} \right] Q_s - \frac{dQ_s}{ds} \right) \right].\end{aligned} \quad (\text{D10})$$

If we again set $s = s_0$ or $s = s_{\text{opt}}$, we get

$$\alpha^{(\text{UB},s')} = \left(\frac{1-p}{p} \right)^{s'} (1-s')Q_{s'}, \quad (\text{D11})$$

$$\beta^{(\text{UB},s')} = \left(\frac{p}{1-p} \right)^{1-s'} s'Q_{s'}, \quad (\text{D12})$$

where s' stands in for either s_0 or s_{opt} . The $s = s_0$ case gives Eqs. (15) and (16) from the main text.

For any value of s , there exists some value of p for which s_{opt} is given by that s value. In other words, we can validly write $p(s_{\text{opt}})$ instead of $s_{\text{opt}}(p)$. This follows from the fact that $p/(1-p)$ can take any positive value, so we can always choose p such that Eq. (D5) is satisfied, and

the convexity of $p^{1-s}(1-p)^s Q_s$ [this can be seen from the decompositions in Eqs. (E4) and (E5)], which means that the point at which Eq. (D5) is satisfied is a minimum.

Using Eq. (D5), we can write

$$\frac{p}{1-p} = \exp \left[Q_{\text{opt}}^{-1} \frac{dQ_s}{ds} \Big|_{s=s_{\text{opt}}} \right], \quad (\text{D13})$$

and thus, can rewrite Eqs. (D11) and (D12), replacing p as our auxiliary parameter with s_{opt} , to get

$$\alpha^{(\text{UB,QCB})} = \left(\exp \left[-s Q_s^{-1} \frac{dQ_s}{ds} \right] (1-s) Q_s \right) \Big|_{s=s_{\text{opt}}}, \quad (\text{D14})$$

$$\beta^{(\text{UB,QCB})} = \left(\exp \left[(1-s) Q_s^{-1} \frac{dQ_s}{ds} \right] s Q_s \right) \Big|_{s=s_{\text{opt}}}. \quad (\text{D15})$$

For consistency with the other equations, we redefine p as s_{opt} and write [Eqs. (19) and (20) in the main text]

$$\alpha^{(\text{UB,QCB})} = \exp \left[-p Q_p^{-1} \frac{dQ_p}{dp} \right] (1-p) Q_p,$$

$$\beta^{(\text{UB,QCB})} = \exp \left[(1-p) Q_p^{-1} \frac{dQ_p}{dp} \right] p Q_p.$$

APPENDIX E: CONNECTION BETWEEN THE OAQCB AND QUANTUM RELATIVE ENTROPY

Ref. [3] points out a connection between the QCB and the QRE, namely that for s_* (the value that minimizes $Q_s(\rho_1, \rho_2)$), the following holds:

$$S(\tau_{s_*} \| \rho_1) = S(\tau_{s_*} \| \rho_2), \quad (\text{E1})$$

$$\tau_s = \frac{\rho_2^s \rho_1^{1-s}}{\text{Tr}[\rho_2^s \rho_1^{1-s}]} = \frac{\rho_2^s \rho_1^{1-s}}{Q_s}. \quad (\text{E2})$$

Here $S(A \| B)$, the QRE between A and B , is defined (in nats) by

$$S(A \| B) = \text{Tr}[A \ln A - A \ln B]. \quad (\text{E3})$$

Note that τ_s is not, in general, a valid quantum state.

In the discrete variable case, we can decompose Q_s as

$$Q_s = \sum_i c_i \lambda_i^s \mu_i^{1-s}, \quad (\text{E4})$$

where c_i , λ_i , and μ_i are all ≥ 0 [3]. The λ_i correspond to eigenvalues of ρ_2 , the μ_i correspond to eigenvalues of ρ_1 , and the c_i correspond to squared overlaps between the eigenvectors of ρ_1 and ρ_2 . We could have written this expression with two separate indices for the λ values and

the μ values (and a nested sum over both), but we have chosen to combine them into the single index i . Similarly, in the continuous-variable case, we can decompose Q_s as

$$Q_s = \int c_x \lambda_x^s \mu_x^{1-s} dx, \quad (\text{E5})$$

where c_x , λ_x , and μ_x are all positive semidefinite functions of x , and where the bounds of the integral may be finite or may be infinite.

By differentiating Eq. (E4) [Eq. (E5) in the continuous-variable case] with regard to s , we get

$$\frac{dQ_s}{ds} = \sum_i c_i \lambda_i^s \mu_i^{1-s} (\ln[\lambda_i] - \ln[\mu_i]) \quad (\text{E6})$$

(with a similar result in the continuous-variable case). We can therefore write

$$S(\tau_p \| \rho_1) - S(\tau_p \| \rho_2) = Q_p^{-1} \frac{dQ_p}{dp}. \quad (\text{E7})$$

For instance, if we want the ratio between $\alpha^{(\text{UB,QCB})}$ and $\beta^{(\text{UB,QCB})}$, for some parameter value p , we can express it in terms of the QRE as

$$\frac{\alpha^{(\text{UB,QCB})}}{\beta^{(\text{UB,QCB})}} = \exp [S(\tau_p \| \rho_1) - S(\tau_p \| \rho_2)] \frac{1-p}{p}. \quad (\text{E8})$$

Taking the limit of Eq. (E6) as $s \rightarrow 0$, we get

$$\frac{dQ_s}{ds} \Big|_{s=0} = \sum_i c_i \mu_i (\ln[\lambda_i] - \ln[\mu_i]) = -S(\rho_1 \| \rho_2), \quad (\text{E9})$$

and taking the limit as $s \rightarrow 1$, we get

$$\frac{dQ_s}{ds} \Big|_{s=1} = \sum_i c_i \lambda_i (\ln[\lambda_i] - \ln[\mu_i]) = S(\rho_2 \| \rho_1). \quad (\text{E10})$$

For some states, the QRE $S(\rho_1 \| \rho_2)$ ($S(\rho_2 \| \rho_1)$) can diverge. This corresponds to some of the λ_i (μ_i) equaling 0. Note that this only occurs for extremal values of s , since we set $0 \ln[0] = 0$. These are also the states for which Q_0 , Q_1 , or both are not equal to 1.

APPENDIX F: GAUSSIAN STATES

The Q_s can be computed for Gaussian states using the formalism developed in Ref. [64]. There it was shown that a Gaussian state $\hat{\rho}$ can be expressed as

$$\hat{\rho} = \frac{e^{-(1/2)(\hat{Q}-u)G(\hat{Q}-u)}}{Z(G)} \equiv \hat{\rho}(G, u), \quad (\text{F1})$$

where \hat{Q} are the quadrature operators, u is the first moment vector, with components $u_i = \text{Tr}[\hat{\rho} \hat{Q}_i]$, the matrix G is

obtained from the covariance matrix, defined by $V_{ij} = \text{Tr}[\hat{\rho}\{\hat{Q}_i - u_i, \hat{Q}_j - u_j\}]/2$ where $\{X, Y\} = XY + YX$, as

$$V \equiv V(G) = \frac{1}{2} \frac{e^{i\Omega G} + \mathbb{1}}{e^{i\Omega G} - \mathbb{1}} i\Omega, \quad e^{i\Omega G} = \frac{W - \mathbb{1}}{W + \mathbb{1}}, \quad (\text{F2})$$

where $W = -2Vi\Omega$ and

$$\begin{aligned} Z(G) &= \det[(e^{i\Omega G/2} - e^{-i\Omega G/2})i\Omega]^{-1/2} \\ &= \sqrt{\det(V + i\Omega/2)}. \end{aligned} \quad (\text{F3})$$

Thanks to the above definitions, the operator $\hat{\rho}^s$ is proportional to a Gaussian state with a rescaled matrix G , namely,

$$\hat{\rho}(G, u)^s = \hat{\rho}(sG, u) \frac{Z(sG)}{Z(G)^s}. \quad (\text{F4})$$

The final ingredient to compute the Q_s is the formula

$$\text{Tr}[\hat{\rho}(G_1, u_1)\hat{\rho}(G_2, u_2)] = \frac{e^{-\delta^T(V(G_1) + V(G_2))^{-1}\delta/2}}{\sqrt{\det[V(G_1) + V(G_2)]}}, \quad (\text{F5})$$

where $\delta = u_1 - u_2$. Suppose now we have two Gaussian states $\hat{\rho}_1$ and $\hat{\rho}_2$ with first moments u_i and covariance matrices V_i . Let G_i be the corresponding matrices in Eq. (F1). Then by mixing the above formulas we get (see also [64,71])

$$\begin{aligned} Q_s &= \text{Tr}[\hat{\rho}_1^s \hat{\rho}_2^{1-s}] \\ &= \frac{Z(sG_1)}{Z(G_1)^s} \frac{Z[(1-s)G_2]}{Z(G_2)^{1-s}} \text{Tr}[\hat{\rho}(sG_1, u_1)\hat{\rho}[(1-s)G_2, u_2]] \\ &= \frac{Z(sG_1)}{Z(G_1)^s} \frac{Z[(1-s)G_2]}{Z(G_2)^{1-s}} \frac{e^{-\delta^T(V_1(s) + V_2(1-s))^{-1}\delta/2}}{\sqrt{\det[V_1(s) + V_2(1-s)]}}, \end{aligned} \quad (\text{F6})$$

where using Eq. (F2) we define the matrices

$$\begin{aligned} V_j(s) &= V(sG_j) = \frac{1}{2} \frac{e^{i\Omega s G_j} + \mathbb{1}}{e^{i\Omega s G_j} - \mathbb{1}} i\Omega \\ &= \frac{1}{2} \frac{[(-2V_j i\Omega - \mathbb{1})/(-2V_j i\Omega + \mathbb{1})]^s + \mathbb{1}}{[(-2V_j i\Omega - \mathbb{1})/(-2V_j i\Omega + \mathbb{1})]^{1-s} - \mathbb{1}} i\Omega. \end{aligned} \quad (\text{F7})$$

This can be simplified by defining

$$W_j(s) = -2V_j(s)i\Omega = \frac{(W_j + \mathbb{1})^s + (W_j - \mathbb{1})^s}{(W_j + \mathbb{1})^s - (W_j - \mathbb{1})^s}. \quad (\text{F8})$$

Note also that $Z(sG_j) = \sqrt{\det[V_j(s) + i\Omega/2]}$, so we get

$$\begin{aligned} Q_s &= \sqrt{\frac{\det[V_1(s) + i\Omega/2]}{\det[V_1 + i\Omega/2]^s} \frac{\det[V_2(1-s) + i\Omega/2]}{\det[V_2 + i\Omega/2]^{1-s}}} \\ &\times \frac{e^{-\delta^T(V_1(s) + V_2(1-s))^{-1}\delta/2}}{\sqrt{\det[V_1(s) + V_2(1-s)]}}. \end{aligned} \quad (\text{F9})$$

Taking the logarithm and using the identity $\log(\det A) = \text{Tr}(\log A)$,

$$\begin{aligned} -2\log Q_s &= \delta^T(V_1(s) + V_2(1-s))^{-1}\delta \\ &+ \text{Tr} \log[V_1(s) + V_2(1-s)] + 2[s \log Z(G_1) \\ &+ (1-s) \log Z(G_2)] - \text{Tr} \log(V_1(s) + i\Omega/2) \\ &- \text{Tr} \log(V_2(1-s) + i\Omega/2). \end{aligned} \quad (\text{F10})$$

To compute derivatives, we note that

$$W'_j(s) = \frac{2(W_j - \mathbb{1})^s (W_j + \mathbb{1})^s}{((W_j - \mathbb{1})^s - (W_j + \mathbb{1})^s)^2} \log \frac{W_j - \mathbb{1}}{W_j + \mathbb{1}} \quad (\text{F11})$$

and $V'_j(s) = -W'_j(s)i\Omega/2$. Moreover, using properties of Fréchet derivatives $\text{Tr}[f'(X(s))] = \text{Tr}[f'(X(s))X'(s)]$, where f' is a function and X a matrix, so

$$\begin{aligned} g_j(s) &= -\partial_s \text{Tr} \log(V_j(s) + i\Omega/2) \\ &= \text{Tr} \left[\frac{(W_j + \mathbb{1})^s}{(W_j - \mathbb{1})^s - (W_j + \mathbb{1})^s} \log \frac{W_j - \mathbb{1}}{W_j + \mathbb{1}} \right]. \end{aligned} \quad (\text{F12})$$

Finally, calling $V_{12}(s) = V_1(s) + V_2(1-s)$ and $Z_i = Z(G_i)$ we can write

$$\begin{aligned} q_s &= -\partial_s \log Q_s \\ &= \log \frac{Z_1}{Z_2} + \frac{g_1(s) - g_2(1-s) + \text{Tr}[V_{12}(s)^{-1}V'_{12}(s)]}{2} \\ &\quad - \frac{1}{2} \delta^T V_{12}(s)^{-1} V'_{12}(s) V_{12}(s)^{-1} \delta. \end{aligned} \quad (\text{F13})$$

APPENDIX G: MULTICOPY SCALING OF THE OAQCB

Since

$$\frac{dQ_{p,(1)}^N}{dp} = NQ_{p,(1)}^{N-1} \frac{dQ_{p,(1)}}{dp}, \quad (\text{G1})$$

we can write [Eqs. (22) and (23) in the main text]

$$\begin{aligned}\alpha_{(N)}^{(\text{UB,QCB})} &= \exp \left[-NpQ_{p,(1)}^{-1} \frac{dQ_{p,(1)}}{dp} \right] (1-p)Q_{p,(1)}^N \\ &= \frac{\left(\alpha_{(1)}^{(\text{UB,QCB})} \right)^N}{(1-p)^{N-1}}, \\ \beta_{(N)}^{(\text{UB,QCB})} &= \exp \left[N(1-p)Q_{p,(1)}^{-1} \frac{dQ_{p,(1)}}{dp} \right] pQ_{p,(1)}^N \\ &= \frac{\left(\beta_{(1)}^{(\text{UB,QCB})} \right)^N}{p^{N-1}}.\end{aligned}$$

We can then use Eqs. (22) and (23) to recover Eqs. (26) and (27) from the main text,

$$\begin{aligned}\gamma_\alpha^{(\text{UB,QCB})} &= pQ_{p,(1)}^{-1} \frac{dQ_{p,(1)}}{dp} - \ln [Q_{p,(1)}], \\ \gamma_\beta^{(\text{UB,QCB})} &= -(1-p)Q_{p,(1)}^{-1} \frac{dQ_{p,(1)}}{dp} - \ln [Q_{p,(1)}].\end{aligned}$$

APPENDIX H: PROOF THAT THE OAQCB SATURATES THE QUANTUM HOEFFDING BOUND

Substituting our expression for $\gamma_\beta^{(\text{UB,QCB})}$ into the expression for $b(r, s)$, we get

$$\begin{aligned}b \left(\gamma_\beta^{(\text{UB,QCB})}, s \right) &= (1-s)^{-1} \left(s(1-p)Q_{p,(1)}^{-1} \frac{dQ_{p,(1)}}{dp} \right. \\ &\quad \left. + s \ln [Q_{p,(1)}] - \ln [Q_{s,(1)}] \right). \quad (\text{H1})\end{aligned}$$

To find the maximum achievable decay rate for α , subject to the constraint that $\gamma_\beta^{(\text{UB,QCB})} \geq r$, we must maximize Eq. (H1) over s (in the range $0 \leq s < 1$). Differentiating with regard to s , and noting that $Q_{p,(1)}^{-1}(dQ_{p,(1)}/dp) = (d/dp)(\ln [Q_{p,(1)}])$, we get

$$\begin{aligned}\frac{db \left(\gamma_\beta^{(\text{UB,QCB})}, s \right)}{ds} &= (1-s)^{-2} \left((1-p) \frac{d}{dp} (\ln [Q_{p,(1)}]) \right. \\ &\quad \left. - (1-s) \frac{d}{ds} (\ln [Q_{s,(1)}]) + \ln [Q_{p,(1)}] - \ln [Q_{s,(1)}] \right). \quad (\text{H2})\end{aligned}$$

Note that the terms in the numerator are either functions only of s or functions only of p . Defining

$$a_x = (1-x) \frac{d}{dx} (\ln [Q_{x,(1)}]) + \ln [Q_{x,(1)}], \quad (\text{H3})$$

we can write

$$\frac{db(\gamma_\beta^{(\text{UB,QCB})}, s)}{ds} = \frac{a_p - a_s}{(1-s)^2}. \quad (\text{H4})$$

We have a turning point in $b(\gamma_\beta^{(\text{UB,QCB})}, s)$ if and only if $a_s = a_p$ (since the denominator is always positive in the range). Therefore, $s = p$ is a turning point. To determine whether this turning point is a global maximum, we differentiate a_s with regard to s . If $(da_s/ds) > 0$ for $0 \leq s < 1$, then $s = p$ is a global maximum. If $(da_s/ds) \geq 0$ for $0 \leq s < 1$ (a slightly weaker condition), then the value of b obtained by setting $s = p$ is still b_{\max} , even if there is an interval of s values in the neighborhood of $s = p$ that also maximize b . We find

$$\frac{da_s}{ds} = (1-s) \frac{d^2}{ds^2} (\ln [Q_{s,(1)}]). \quad (\text{H5})$$

Since $(1-s) > 0$ in our range, the condition for $s = p$ to maximize b reduces to the requirement that the second differential of $\ln [Q_{s,(1)}]$ is positive semidefinite. We therefore need to show that the function Q_s is logarithmically convex (log-convex) in s [72]. This is a stricter condition than convexity, and means that $\ln Q_s$ is also convex (as well as Q_s). The second derivative of any convex function is nonnegative, so it suffices to show that Q_s is log-convex.

The condition for a function, f , to be log-convex is

$$f(tx_1 + (1-t)x_2) \leq f(x_1)^t f(x_2)^{1-t} \quad (\text{H6})$$

for $0 \leq t \leq 1$ [72]. From Ref. [72], we have that the set of log-convex functions (referred to in Ref. [72] as superconvex functions) is closed under addition. This means that a linear combination of log-convex functions is also log-convex. Ref. [72] also shows that if every member of a sequence of functions is log-convex, the limit of the supremum of the sequence (limsup) is also log-convex.

First, let us consider the discrete variable case. Recall Eq. (E4) (repeated here for convenience), which tells us that for discrete variables, we can decompose Q_s as

$$Q_s = \sum_i c_i \lambda_i^s \mu_i^{1-s}.$$

Let $f(s)$ be the function $s \mapsto c \lambda^s \mu^{1-s}$ for some positive numbers c , λ , and μ . Here $f(s)$ is log-convex,

$$\begin{aligned}f(tx_1 + (1-t)x_2) &= c \lambda^{tx_1 + (1-t)x_2} \mu^{1-(tx_1 + (1-t)x_2)} \\ &= (c^t \lambda^{tx_1} \mu^{t(1-x_1)}) \\ &\quad \times (c^{1-t} \lambda^{(1-t)x_1} \mu^{(1-t)(1-x_1)}) \\ &= f(x_1)^t f(x_2)^{1-t}. \quad (\text{H7})\end{aligned}$$

Since Q_s is a sum of such functions, it is also log-convex. This is true even if the sum is unbounded and i takes values up to ∞ .

Let us extend this result to continuous-variable states. We can use the fact that the set of log-convex functions is closed under limsup. Suppose that, for any pair of continuous-variable states, we can define a sequence of log-convex approximations to Q_s , $Q_s^{(i)}$, so that the supremum of the bounds tends to Q_s in the limit of $i \rightarrow \infty$. Then, Q_s must also be log-convex. One subtlety is that the $Q_s^{(i)}$ must all be lower bounds, so that Q_s is the limsup, rather than just the limit.

Recall Eq. (E5) (repeated here for convenience), which decomposes Q_s as

$$Q_s = \int c_x \lambda_x^s \mu_x^{1-s} dx.$$

Let us initially assume that $0 \leq x < R$ for finite R (i.e., the integral has finite bounds). We can then define our approximations, $Q_s^{(i)}$, as

$$\begin{aligned} Q_s^{(i)} &= \Delta_i \sum_{j=1}^i \left(\inf_{(j-1)\Delta_i \leq x < j\Delta_i} c_x \right) \left(\inf_{(j-1)\Delta_i \leq x < j\Delta_i} \rho_x \right)^s \\ &\times \left(\inf_{(j-1)\Delta_i \leq x < j\Delta_i} \sigma_x \right)^{1-s}, \end{aligned} \quad (\text{H8})$$

where $\Delta_i = R/i$. This is a kind of lower Riemann sum, and it is clear that, for any finite number of samples, i , $Q_s^{(i)}$ both lower bounds Q_s and is log-convex. Taking the limit as $i \rightarrow \infty$ and, therefore, as $\Delta_i \rightarrow 0$, we get Q_s . To extend to an infinite domain for x , we truncate the function outside the finite domain $0 \leq x < R$, take the limit as $i \rightarrow \infty$, and then take the limit again as $R \rightarrow \infty$.

We can therefore write

$$b_{\max}(\gamma_\beta^{(\text{UB,QCB})}) = b(\gamma_\beta^{(\text{UB,QCB})}, p) = \gamma_\alpha^{(\text{UB,QCB})}, \quad (\text{H9})$$

showing that the OAQCB achieves the best possible scaling, according to the quantum Hoeffding bound.

Note that we assume that $\gamma_\beta^{(\text{UB,QCB})}$ lies in the range $0 < \gamma_\beta^{(\text{UB,QCB})} < S(\rho_1 \| \rho_2)$. We now show that this always holds, except at the extremal points ($p = 0$ and $p = 1$), at which the quantum Stein's lemma holds.

APPENDIX I: DERIVATION OF RESULTS SHOWING THE OAQCB SATURATES THE QUANTUM STEIN'S LEMMA

Equations (29) and (30) in the main text come from applying Eqs. (E9) and (E10) when taking the limits.

We show that $\gamma_\beta^{(\text{UB,QCB})}$ is a nonincreasing function of p by rewriting Eq. (27) as

$$\gamma_\beta^{(\text{UB,QCB})} = -(1-p) \frac{d}{dp} (\ln[Q_{p,(1)}]) - \ln[Q_{p,(1)}] \quad (\text{I1})$$

and differentiating it, to get

$$\frac{d\gamma_\beta^{(\text{UB,QCB})}}{dp} = -(1-p) \frac{d^2}{dp^2} (\ln[Q_{p,(1)}]). \quad (\text{I2})$$

Since Q_s is log-convex, the right-hand side of Eq. (I2) is negative semidefinite, and so $\gamma_\beta^{(\text{UB,QCB})}$ is a nonincreasing function of p .

APPENDIX J: ERROR RATES FOR NONADAPTIVE MEASUREMENT SEQUENCES

Consider the measurement sequences described in the main text. The errors for each case can be calculated using Eqs. (7) and (8), and are given by

$$\alpha^{(\text{A})} = 1 - (1 - \alpha^{(\text{LB}, F_{(1)})})^3, \quad (\text{J1})$$

$$\beta^{(\text{A})} = (\beta^{(\text{LB}, F_{(1)})})^3, \quad (\text{J2})$$

for case A,

$$\alpha^{(\text{B})} = 3(\alpha^{(\text{LB}, F_{(1)})})^2 - 2(\alpha^{(\text{LB}, F_{(1)})})^3, \quad (\text{J3})$$

$$\beta^{(\text{B})} = 3(\beta^{(\text{LB}, F_{(1)})})^2 - 2(\beta^{(\text{LB}, F_{(1)})})^3, \quad (\text{J4})$$

for case B, and

$$\alpha^{(\text{C})} = (\alpha^{(\text{LB}, F_{(1)})})^3, \quad (\text{J5})$$

$$\beta^{(\text{C})} = 1 - (1 - \beta^{(\text{LB}, F_{(1)})})^3. \quad (\text{J6})$$

for case C. All three cases differ from the optimum,

$$\alpha^{(\text{opt})} = \alpha^{(\text{LB}, F_{(3)} = F_{(1)}^3)}, \quad \beta^{(\text{opt})} = \beta^{(\text{LB}, F_{(3)} = F_{(1)}^3)}, \quad (\text{J7})$$

except at the points given by parameter values $p = 0$ and $p = 1$. This is illustrated in Fig. 4.

APPENDIX K: ERROR RATES FOR ADAPTIVE MEASUREMENT SEQUENCES

Let us consider the error rates for the adaptive measurement sequence described in the main text (for states with two subsystems).

Recall that we carry out an optimal measurement, with parameter value p_0 , on the first subsystem. If this measurement tells us that the state is $\rho_{1,1}$, we carry out another optimal measurement with parameter value p_1 , otherwise we carry out a measurement on the second subsystem with parameter value p_2 . We use only the result of the second measurement to decide which state we have.

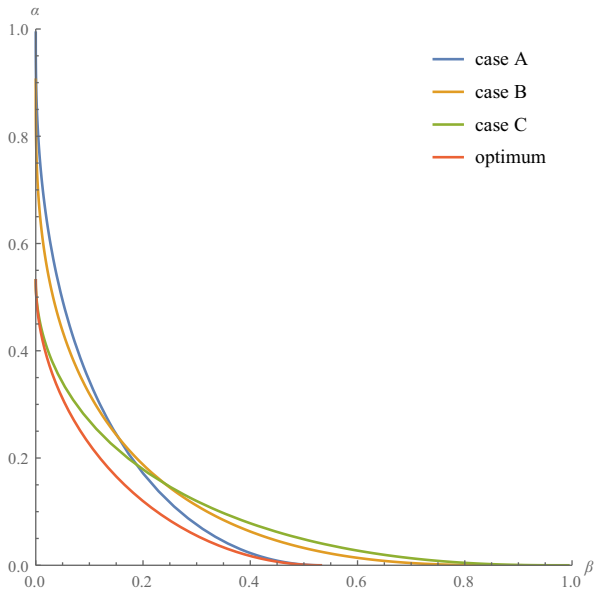


FIG. 4. Type I and II errors for discriminating between a pair of pure, three-copy states, for which the single-copy fidelity is 0.9. In cases A, B, and C the same (optimal) single-copy measurement is carried out on each subsystem of the state. The cases differ in how we determine the identity of the state from the measurement results. All three methods are worse than the optimal joint measurement, denoted “optimum” (except at the two points where the optimal curve meets the axes). Case B—where the state is determined using the majority vote—is never better than both cases A and C.

The Type I error for the sequence, α_{seq} , is given by

$$\begin{aligned} \alpha_{\text{seq}} = & (1 - \alpha^{(\text{LB}, F_1)}[p_0])\alpha^{(\text{LB}, F_2)}[p_1] \\ & + \alpha^{(\text{LB}, F_1)}[p_0]\alpha^{(\text{LB}, F_2)}[p_2], \end{aligned} \quad (\text{K1})$$

and the Type II error, β_{seq} , is given by

$$\begin{aligned} \beta_{\text{seq}} = & \beta^{(\text{LB}, F_1)}[p_0]\beta^{(\text{LB}, F_2)}[p_1] \\ & + (1 - \beta^{(\text{LB}, F_1)}[p_0])\beta^{(\text{LB}, F_2)}[p_2]. \end{aligned} \quad (\text{K2})$$

We set [Eq. (31) in the main text]

$$p_1^{\mp} = \frac{1}{2} \left(1 \mp \sqrt{1 - 4p_0(1 - p_0)F_1^2} \right).$$

Substituting these values into Eqs. (K1) and (K2) [and using Eqs. (7) and (8)], we get

$$\alpha_{\text{seq}} = \frac{2(1 - p_0)F_1^2F_2^2 - 1 + \sqrt{1 - 4p_0(1 - p_0)F_1^2F_2^2}}{2\sqrt{1 - 4p_0(1 - p_0)F_1^2F_2^2}}, \quad (\text{K3})$$

$$\beta_{\text{seq}} = \frac{2p_0F_1^2F_2^2 - 1 + \sqrt{1 - 4p_0(1 - p_0)F_1^2F_2^2}}{2\sqrt{1 - 4p_0(1 - p_0)F_1^2F_2^2}}. \quad (\text{K4})$$

Now note that

$$\alpha_{\text{seq}} = \alpha^{(\text{LB}, F_1F_2)}[p_0], \quad \beta_{\text{seq}} = \beta^{(\text{LB}, F_1F_2)}[p_0], \quad (\text{K5})$$

so this measurement sequence achieves the optimal errors for discriminating between states with a fidelity of F_1F_2 .

APPENDIX L: COMPARISON WITH EXISTING TECHNIQUES AND BOUNDS

It is possible to calculate the exact ROC using Eq. (3) from the main text. With this in mind, we might ask why we need to use the bounds presented in the main text.

Calculating the eigendecomposition of $(1 - p)\rho_2 - p\rho_1$ [in order to apply Eq. (3)] can be difficult for high-dimensional states and continuous-variable states. Even for Gaussian states (a class of CV states for which calculations are often significantly simpler), the optimal measurement is non-Gaussian, so there is no known simple way to calculate the ROC directly from the first and second moments.

Suppose we only want to numerically find specific points on the ROC. For discrete variable states, we can formulate the problem of minimizing one type of error with the other fixed as a semidefinite programming problem. Specifically, we can express it as

$$\begin{aligned} \text{minimize: } & 1 - \text{Tr}[X\rho_2], \\ \text{subject to: } & X\rho_1 - \alpha\mathcal{I} \geq 0, \\ & X \in \mathcal{H}, \end{aligned}$$

where \mathcal{H} is the set of Hermitian matrices with the same dimension as (the matrix representation of) ρ_2 . The optimal X will be the same POVM given by Eq. (3). However, the size of the search space (\mathcal{H}) increases with the dimension of the states, so that for high-dimensional states, finding the optimal measurement this way becomes very difficult. For continuous-variable states, it is not possible to use this method at all (without some truncation), since they are infinite dimensional.

Whilst it is also true that calculating the fidelity or Q_p , in order to apply the bounds from the main text, also becomes more difficult for higher-dimensional discrete variable states, in many scenarios these quantities are much easier to calculate. For instance, if the states take tensor-product form (e.g., if we have multiple copies of the same state in both scenarios), we can calculate the fidelity or Q_p

on each pair of subsystems individually, and then apply the multiplicativity of fidelity or Q_p over tensor products. For the OAQCB, we can write the following equation for an N -partite system [similar to Eqs. (22) and (23) in the main text]:

$$\alpha^{(\text{UB,QCB})} = \frac{\prod_{i=1}^N \alpha_{(i)}^{(\text{UB,QCB})}}{(1-p)^{N-1}}, \quad (\text{L1})$$

$$\beta^{(\text{UB,QCB})} = \frac{\prod_{i=1}^N \beta_{(i)}^{(\text{UB,QCB})}}{p^{N-1}}. \quad (\text{L2})$$

Here $\alpha_{(i)}^{(\text{UB,QCB})}$ and $\beta_{(i)}^{(\text{UB,QCB})}$ comprise the OAQCB calculated for the i th subsystem. In the CV case, if we have Gaussian states, both the fidelity [64] and Q_p [65] can be calculated directly from the first and second moments.

Conversely, the trace norm for tensor-product states cannot be calculated using the tensor products on individual subsystems. Similarly, if we want to find the minimum errors numerically, using semidefinite programming, the operators that we minimize over will have the dimension of the entire system. If both states are pure, we can constrain the possible measurements to be convex combinations of measurements in tensor-product form (see Sec. VI in the main text), but this simplification still does not reduce the problem to minimizing over each subsystem individually. This is clear from the fact that to find a single point on the ROC for discriminating between two pure bipartite systems, one must find two points on the ROC for one of the subsystems, since the optimal measurement can be expressed as an adaptive sequence of measurements on individual subsystems.

If we have a large number of copies of the same state, we can apply the quantum Stein's lemma or the quantum Hoeffding bound to compute the optimal errors. However, these are only tight asymptotically (i.e., for large numbers of copies, N), because they govern how quickly the errors exponentially decay. They do not tell us about any subexponential terms (such as constant prefactors) that the errors may have. Whilst these terms may become negligible for large N , there are situations in which N is small enough that we still care about subexponential terms, but still large enough that it is difficult to calculate the exact error values. Recall that the dimension of the states grows exponentially with N , so N does not need to be very large for it to be difficult to calculate the ROC exactly.

One task that constitutes an interesting extension to the problem of discriminating between N copies of one of two states is that of discriminating between two different sequences of N states. In such a scenario, it may not be possible to use the quantum Stein's lemma or the quantum Hoeffding bound at all. For large N , it would also be difficult to calculate the exact errors using the quantum Neyman-Pearson relation. For instance, consider

sequences of states whose n th elements are of the form

$$\rho_1^n = \begin{pmatrix} \frac{1}{2} & \frac{1}{4n} \\ \frac{1}{4n} & \frac{1}{2} \end{pmatrix}, \quad \rho_2^n = \begin{pmatrix} \frac{1}{2} & -\frac{1}{4n} \\ -\frac{1}{4n} & \frac{1}{2} \end{pmatrix}. \quad (\text{L3})$$

This could model, for instance, a situation in which we can interact with a system multiple times, but each time the interaction is weaker or noisier than the previous. In this scenario, it is not possible to use the quantum Stein's lemma to bound the asymptotic discrimination error. However, we can easily calculate the fidelity and can even take the limit as $N \rightarrow \infty$. We can also calculate the OAQCB for any N and for $N \rightarrow \infty$.

There are therefore two main scenarios in which the bounds we present are useful. The first is when dealing with CV states (and particularly Gaussian states), since it can be difficult to calculate the exact errors, even in the single-copy case. The second is for tensor-product states that are too large to easily calculate the exact errors for, but for which we still care about the exact values, rather than the asymptotic error exponents (or for which the copies are nonidentical).

The hypothesis testing relative entropy [57], defined as

$$D_H^\epsilon(\rho\|\sigma) = -\log_2 \inf_{\substack{0 \leq Q \leq I, \\ \text{Tr}[Q\rho] \geq 1-\epsilon}} \text{Tr}[Q\sigma], \quad (\text{L4})$$

is another way of expressing the ROC. By definition,

$$D_H^{\alpha^*}(\rho_1\|\rho_2) = -\log_2 \beta^*, \quad D_H^{\beta^*}(\rho_2\|\rho_1) = -\log_2 \alpha^*. \quad (\text{L5})$$

From Ref. [57], we have the following upper bound on the hypothesis testing relative entropy:

$$D_H^\epsilon(\rho\|\sigma) \leq \frac{S(\rho\|\sigma) + h(\epsilon)}{1-\epsilon}. \quad (\text{L6})$$

Here h is the binary entropy function, defined by

$$h(\epsilon) = -\epsilon \log_2(\epsilon) - (1-\epsilon) \log_2(1-\epsilon), \quad (\text{L7})$$

and S is the standard quantum relative entropy, but expressed in bits (rather than nats, as was done previously), for consistency with Ref. [57]. This leads to the following two different lower bounds on the ROC:

$$\alpha^* \geq 2^{-[S(\rho_2\|\rho_1) + h(\beta^*)]/(1-\beta^*)}, \quad (\text{L8})$$

$$\beta^* \geq 2^{-[S(\rho_1\|\rho_2) + h(\alpha^*)]/(1-\alpha^*)}. \quad (\text{L9})$$

Note that $S(\rho_2\|\rho_1)$ and $S(\rho_1\|\rho_2)$ are generally different, so these bounds are not mirror images of each other.

If the QRE $S(\rho_2\|\rho_1)$ is not infinite (i.e., if the support of ρ_2 lies entirely within the support of ρ_1), then the bound defined by Eq. (L8) runs between the points $(0, 2^{-S(\rho_2\|\rho_1)})$ and $(1, 0)$ [since this bound is not symmetric, we specify that points are written in the form (β, α)]. Crucially, this means that, for any $\beta < 1$, α will be nonzero, and so this bound will beat the fidelity-based lower bound over some range of β values. If $S(\rho_2\|\rho_1)$ diverges then the bound is trivial (stating that, for any β^* , $\alpha^* \geq 0$). Similarly, if $S(\rho_1\|\rho_2)$ does not diverge, the bound defined by Eq. (L9) runs between the points $(0, 1)$ and $(2^{-S(\rho_2\|\rho_1)}, 0)$, and so this bound will beat the fidelity-based lower bound over some range of α values.

There is no contradiction with the fact that the fidelity-based lower bound is exact for pure states, since $S(\rho_1\|\rho_2)$ and $S(\rho_1\|\rho_2)$ both diverge for pure states [$S(\rho_1\|\rho_2)$ diverges if ρ_2 is pure and $S(\rho_2\|\rho_1)$ diverges if ρ_1 is pure]. In fact, if the support of ρ_1 lies within the support of ρ_2 , it is not possible to set $\alpha = 0$ without setting $\beta = 1$ (and vice versa, if the support of ρ_2 lies within the support of ρ_1), so it is not surprising that there exists a tighter bound than the fidelity-based lower bound for small α or β in such cases.

The QRE is not a distance metric, and even a small (in terms of trace norm) change in the states ρ_1 and ρ_2 can result in one or both of the relative entropies varying greatly or even diverging. If the states are not diagonalizable in the same basis and if either of the states is not full rank, at least one of the relative entropies will diverge (and the corresponding bound will become trivial).

Finally, note that $F^2 \geq 2^{-S}$, where S is either $S(\rho_1\|\rho_2)$ or $S(\rho_1\|\rho_2)$ [73], so the fidelity-based lower bound will always (except in the $F^2 = 2^{-S}$ case) beat the bounds in Eqs. (L8) and (L9) over some range of values (but over a different range for each bound). If both $S(\rho_1\|\rho_2)$ and $S(\rho_2\|\rho_1)$ are close to F^2 , it may be the case that by choosing whichever is tighter of Eqs. (L8) and (L9), we can beat the fidelity-based lower bound over the entire range. However, we find numerically that for states with a sufficiently high fidelity (more than approximately 0.94), the fidelity-based bound beats the bounds based on the QRE over some range (α and β not close to 0) even when $F^2 = 2^{-S(\rho_1\|\rho_2)} = 2^{-S(\rho_2\|\rho_1)}$.

- [5] A. Karsa, G. Spedalieri, Q. Zhuang, and S. Pirandola, Quantum illumination with a generic Gaussian source, *Phys. Rev. Res.* **2**, 023414 (2020).
- [6] S. Lloyd, Enhanced sensitivity of photodetection via quantum illumination, *Science* **321**, 1463 (2008).
- [7] S.-H. Tan, B. I. Erkmen, V. Giovannetti, S. Guha, S. Lloyd, L. Maccone, S. Pirandola, and J. H. Shapiro, Quantum Illumination with Gaussian States, *Phys. Rev. Lett.* **101**, 253601 (2008).
- [8] J. H. Shapiro and S. Lloyd, Quantum illumination versus coherent-state target detection, *New J. Phys.* **11**, 063045 (2009).
- [9] Q. Zhuang, Z. Zhang, and J. H. Shapiro, Optimum Mixed-State Discrimination for Noisy Entanglement-Enhanced Sensing, *Phys. Rev. Lett.* **118**, 040801 (2017).
- [10] Q. Zhuang, Z. Zhang, and J. H. Shapiro, Entanglement-enhanced Neyman-Pearson target detection using quantum illumination, *J. Opt. Soc. Am. B* **34**, 1567 (2017).
- [11] S. Barzanjeh, S. Guha, C. Weedbrook, D. Vitali, J. H. Shapiro, and S. Pirandola, Microwave Quantum Illumination, *Phys. Rev. Lett.* **114**, 080503 (2015).
- [12] S. Guha and B. I. Erkmen, Gaussian-state quantum-illumination receivers for target detection, *Phys. Rev. A* **80**, 052310 (2009).
- [13] B. Xiong, X. Li, X.-Y. Wang, and L. Zhou, Improve microwave quantum illumination via optical parametric amplifier, *Ann. Phys. (N. Y.)* **385**, 757 (2017).
- [14] M. Sanz, U. Las Heras, J. J. García-Ripoll, E. Solano, and R. Di Candia, Quantum Estimation Methods for Quantum Illumination, *Phys. Rev. Lett.* **118**, 070803 (2017).
- [15] C. Weedbrook, S. Pirandola, J. Thompson, V. Vedral, and M. Gu, How discord underlies the noise resilience of quantum illumination, *New J. Phys.* **18**, 043027 (2016).
- [16] S. Ragy, I. R. Berchera, I. P. Degiovanni, S. Olivares, M. G. A. Paris, G. Adesso, and M. Genovese, Quantifying the source of enhancement in experimental continuous variable quantum illumination, *J. Opt. Soc. Am. B* **31**, 2045 (2014).
- [17] M. M. Wilde, M. Tomamichel, S. Lloyd, and M. Berta, Gaussian Hypothesis Testing and Quantum Illumination, *Phys. Rev. Lett.* **119**, 120501 (2017).
- [18] G. De Palma and J. Borregaard, Minimum error probability of quantum illumination, *Phys. Rev. A* **98**, 012101 (2018).
- [19] E. D. Lopaeva, I. Ruo Berchera, I. P. Degiovanni, S. Olivares, G. Brida, and M. Genovese, Experimental Realization of Quantum Illumination, *Phys. Rev. Lett.* **110**, 153603 (2013).
- [20] A. Meda, E. Losero, N. Samantaray, F. Scafirimuto, S. Pradyumna, A. Avella, I. Ruo-Berchera, and M. Genovese, Photon-number correlation for quantum enhanced imaging and sensing, *J. Opt.* **19**, 094002 (2017).
- [21] Z. Zhang, M. Tengner, T. Zhong, F. N. C. Wong, and J. H. Shapiro, Entanglement's Benefit Survives an Entanglement-Breaking Channel, *Phys. Rev. Lett.* **111**, 010501 (2013).
- [22] Z. Zhang, S. Mouradian, F. N. C. Wong, and J. H. Shapiro, Entanglement-Enhanced Sensing in a Lossy and Noisy Environment, *Phys. Rev. Lett.* **114**, 110506 (2015).
- [23] S. Pirandola, Quantum Reading of a Classical Digital Memory, *Phys. Rev. Lett.* **106**, 090504 (2011).

- [24] C. Lupo, S. Pirandola, V. Giovannetti, and S. Mancini, Quantum reading capacity under thermal and correlated noise, *Phys. Rev. A* **87**, 062310 (2013).
- [25] G. Spedalieri, Cryptographic aspects of quantum reading, *Entropy* **17**, 2218 (2015).
- [26] S. Pirandola, C. Lupo, V. Giovannetti, S. Mancini, and S. L. Braunstein, Quantum reading capacity, *New J. Phys.* **13**, 113012 (2011).
- [27] S. Guha and J. H. Shapiro, Reading boundless error-free bits using a single photon, *Phys. Rev. A* **87**, 062306 (2013).
- [28] R. Nair, Discriminating quantum-optical beam-splitter channels with number-diagonal signal states: Applications to quantum reading and target detection, *Phys. Rev. A* **84**, 032312 (2011).
- [29] R. Nair and B. J. Yen, Optimal Quantum States for Image Sensing in Loss, *Phys. Rev. Lett.* **107**, 193602 (2011).
- [30] J. P. Tej, A. R. Usha Devi, and A. K. Rajagopal, Quantum reading of digital memory with non-Gaussian entangled light, *Phys. Rev. A* **87**, 052308 (2013).
- [31] A. Bisio, M. Dall'Arno, and G. M. D'Ariano, Tradeoff between energy and error in the discrimination of quantum-optical devices, *Phys. Rev. A* **84**, 012310 (2011).
- [32] M. Dall'Arno, A. Bisio, G. M. D'Ariano, M. Miková, M. Ježek, and M. Dušek, Experimental implementation of unambiguous quantum reading, *Phys. Rev. A* **85**, 012308 (2012).
- [33] C. Invernizzi, M. G. A. Paris, and S. Pirandola, Optimal detection of losses by thermal probes, *Phys. Rev. A* **84**, 022334 (2011).
- [34] M. Dall'arno, A. Bisio, and G. Mauro D'ariano, Ideal quantum reading of optical memories, *Int. J. Quantum Inform.* **10**, 1241010 (2012).
- [35] W. Roga, D. Buono, and F. Illuminati, Device-independent quantum reading and noise-assisted quantum transmitters, *New J. Phys.* **17**, 013031 (2015).
- [36] L. Banchi, Q. Zhuang, and S. Pirandola, Quantum-Enhanced Barcode Decoding and Pattern Recognition, *Phys. Rev. Appl.* **14**, 064026 (2020).
- [37] G. Spedalieri, L. Piersimoni, O. Laurino, S. L. Braunstein, and S. Pirandola, Detecting and tracking bacteria with quantum light, *Phys. Rev. Res.* **2**, 043260 (2020).
- [38] M. Tsang, R. Nair, and X.-M. Lu, Quantum Theory of Superresolution for Two Incoherent Optical Point Sources, *Phys. Rev. X* **6**, 031033 (2016).
- [39] C. Lupo and S. Pirandola, Ultimate Precision Bound of Quantum and Subwavelength Imaging, *Phys. Rev. Lett.* **117**, 190802 (2016).
- [40] R. Nair and M. Tsang, Far-Field Superresolution of Thermal Electromagnetic Sources at the Quantum Limit, *Phys. Rev. Lett.* **117**, 190801 (2016).
- [41] R. Kerviche, S. Guha, and A. Ashok, Fundamental limit of resolving two point sources limited by an arbitrary point spread function, *ArXiv:1701.04913* (2017).
- [42] J. Rehacek, M. Paúr, B. Stoklasa, Z. Hradil, and L. L. Sánchez-Soto, Optimal measurements for resolution beyond the Rayleigh limit, *Opt. Lett.* **42**, 231 (2017).
- [43] F. Yang, R. Nair, M. Tsang, C. Simon, and A. I. Lvovsky, Fisher information for far-field linear optical superresolution via homodyne or heterodyne detection in a higher-order local oscillator mode, *Phys. Rev. A* **96**, 063829 (2017).
- [44] X.-M. Lu, H. Krovi, R. Nair, S. Guha, and J. H. Shapiro, Quantum-optimal detection of one-versus-two incoherent optical sources with arbitrary separation, *Npj Quantum Inf.* **4**, 1 (2018).
- [45] Z. S. Tang, K. Durak, and A. Ling, Fault-tolerant and finite-error localization for point emitters within the diffraction limit, *Opt. Express* **24**, 22004 (2016).
- [46] R. Nair and M. Tsang, Interferometric superlocalization of two incoherent optical point sources, *Opt. Express* **24**, 3684 (2016).
- [47] F. Yang, A. Tashchilina, E. S. Moiseev, C. Simon, and A. I. Lvovsky, Far-field linear optical superresolution via heterodyne detection in a higher-order local oscillator mode, *Optica* **3**, 1148 (2016).
- [48] W.-K. Tham, H. Ferretti, and A. M. Steinberg, Beating Rayleigh's Curse by Imaging Using Phase Information, *Phys. Rev. Lett.* **118**, 070801 (2017).
- [49] M. Paúr, B. Stoklasa, Z. Hradil, L. L. Sánchez-Soto, and J. Rehacek, Achieving the ultimate optical resolution, *Optica* **3**, 1144 (2016).
- [50] D. Gatto Monticone, K. Katamadze, P. Traina, E. Moreva, J. Forneris, I. Ruo-Berchera, P. Olivero, I. P. Degiovanni, G. Brida, and M. Genovese, Beating the Abbe Diffraction Limit in Confocal Microscopy via Nonclassical Photon Statistics, *Phys. Rev. Lett.* **113**, 143602 (2014).
- [51] A. Classen, F. Waldmann, S. Giebel, R. Schneider, D. Bhatti, T. Mehringer, and J. von Zanthier, Superresolving Imaging of Arbitrary One-Dimensional Arrays of Thermal Light Sources Using Multiphoton Interference, *Phys. Rev. Lett.* **117**, 253601 (2016).
- [52] M. Tsang, Quantum Imaging beyond the Diffraction Limit by Optical Centroid Measurements, *Phys. Rev. Lett.* **102**, 253601 (2009).
- [53] L. A. Rozema, J. D. Bateman, D. H. Mahler, R. Okamoto, A. Feizpour, A. Hayat, and A. M. Steinberg, Scalable Spatial Superresolution Using Entangled Photons, *Phys. Rev. Lett.* **112**, 223602 (2014).
- [54] S. Pirandola, *et al.*, Advances in quantum cryptography, *Adv. Opt. Photonics* **12**, 1012 (2020).
- [55] S. Pirandola, R. Laurenza, C. Ottaviani, and L. Banchi, Fundamental limits of repeaterless quantum communications, *Nat. Commun.* **8**, 1 (2017).
- [56] K. M. R. Audenaert, M. Mosonyi, and F. Verstraete, Quantum state discrimination bounds for finite sample size, *J. Math. Phys.* **53**, 122205 (2012).
- [57] L. Wang and R. Renner, One-Shot Classical-Quantum Capacity and Hypothesis Testing, *Phys. Rev. Lett.* **108**, 200501 (2012).
- [58] F. Hiai and D. Petz, The proper formula for relative entropy and its asymptotics in quantum probability, *Commun. Math. Phys.* **143**, 99 (1991).
- [59] T. Ogawa and H. Nagaoka, Strong converse and Stein's lemma in quantum hypothesis testing, *IEEE Trans. Inf. Theory* **46**, 2428 (2000).
- [60] K. Li, Second-order asymptotics for quantum hypothesis testing, *Ann. Stat.* **42**, 171 (2014).
- [61] M. Berta, F. G. S. L. Brandão, and C. Hirche, On composite quantum hypothesis testing, *Commun. Math. Phys.* **385**, 55 (2021).

- [62] H. Nagaoka, The converse part of the theorem for quantum Hoeffding bound, [ArXiv:quant-ph/0611289](https://arxiv.org/abs/quant-ph/0611289), 2006.
- [63] M. Hayashi, Error exponent in asymmetric quantum hypothesis testing and its application to classical-quantum channel coding, *Phys. Rev. A* **76**, 062301 (2007).
- [64] L. Banchi, S. L. Braunstein, and S. Pirandola, Quantum Fidelity for Arbitrary Gaussian States, *Phys. Rev. Lett.* **115**, 260501 (2015).
- [65] S. Pirandola and S. Lloyd, Computable bounds for the discrimination of Gaussian states, *Phys. Rev. A* **78**, 012331 (2008).
- [66] See Supplemental Material at <http://link.aps.org/supplemental/10.1103/PhysRevApplied.19.054030> for an implementation of the bounds in Mathematica and the code used to generate Figs. 2–4.
- [67] L. Banchi, J. Pereira, S. Lloyd, and S. Pirandola, Convex optimization of programmable quantum computers, *npj Quantum Inf.* **6**, 42 (2020).
- [68] C. Weedbrook, S. Pirandola, R. García-Patrón, N. J. Cerf, T. C. Ralph, J. H. Shapiro, and S. Lloyd, Gaussian quantum information, *Rev. Mod. Phys.* **84**, 621 (2012).
- [69] A. Acín, E. Bagan, M. Baig, L. Masanes, and R. Muñoz-Tapia, Multiple-copy two-state discrimination with individual measurements, *Phys. Rev. A* **71**, 032338 (2005).
- [70] S. Branden, M. Lian, K. D. Stubbs, N. Rengaswamy, and H. D. Pfister, Adaptive procedures for discriminating between arbitrary tensor-product quantum states, *Phys. Rev. A* **106**, 012408 (2022).
- [71] K. P. Seshadreesan, L. Lami, and M. M. Wilde, Rényi relative entropies of quantum gaussian states, *J. Math. Phys.* **59**, 072204 (2018).
- [72] J. F. C. Kingman, A convexity property of positive matrices, *Q. J. Math.* **12**, 283 (1961).
- [73] K. M. R. Audenaert, Comparisons between quantum state distinguishability measures, *Quantum Inf. Comput.* **14**, 31 (2014).